



Cite this: *Phys. Chem. Chem. Phys.*, 2025, 27, 18935

# Investigating dose rate effects and reactive species formation in irradiated multilayer films – part 1 EVA/EVOH/EVA†

Blanche Krieguer,<sup>a</sup> <sup>abc</sup> Samuel Dorey,<sup>a</sup> <sup>a</sup> Nathalie Dupuy,<sup>b</sup> <sup>c</sup> Fabien Girard,<sup>c</sup> Florent Kuntz,<sup>d</sup> <sup>d</sup> Nicolas Ludwig <sup>d</sup> and Sylvain R. A. Marque <sup>b</sup>

This study investigates the effects of gamma rays, X-rays, and electron beams on ethylene vinyl acetate (EVA) multilayer films, commonly used in biotechnological applications. Electron spin resonance (ESR) analysis showed that irradiation generates unstable hydroxyalkyl radicals, quantifiable one day post-exposure, with concentrations decreasing within nine days, and with similar kinetics observed across all three irradiation technologies. The research focuses on dose rate impacts, which significantly influence polymer properties. Reactive species like hydrogen peroxide and hydroxyl radicals, generated during irradiation, can affect protein function through methionine oxidation. Advanced analytical techniques reveal that the dose rate significantly impacted the levels of reactive species, impacting the film's structural integrity and chemical stability comparably. Gamma irradiation generates more oxidative species. The study concludes that dose rate is crucial in methionine sulfoxide generation, with longer exposure leading to increased concentrations, particularly in gamma irradiation. These findings underscore the importance of considering dose rate and irradiation technology to optimize the stability and performance of multilayer films.

Received 29th October 2024,  
Accepted 6th June 2025

DOI: 10.1039/d4cp04152f

[rsc.li/pccp](http://rsc.li/pccp)

## Introduction

Single-use plastic bags are extensively used in the biotechnological and biopharmaceutical industries for storing, shipping, and preparing intermediates, biopharmaceutical preparations, solutions, and final products.<sup>1,2</sup> These bags are typically constructed from multilayer films, such as polyethylene polyvinyl acetate/polyethylene vinyl alcohol/polyethylene polyvinyl acetate (EVA/EVOH/EVA), selected for their barrier protection and flexibility to ensure the integrity of the contents. To eliminate microorganisms, these single-use plastic bags require sterilization, usually within a dose range of 25–45 kGy.<sup>3,4</sup> Currently, gamma radiation is the most prevalent sterilization method for pharmaceutical devices. However, the growing production of biopharmaceutical products and concerns about the future capacity of gamma radiation sterilization have prompted the

exploration of alternative methods, such as electron beam (e-beam) and X-ray irradiation.<sup>5–12</sup>

Electron-beam irradiation is a continuous process that employs an electron accelerator to convert electricity into a radiation beam.<sup>13</sup> These accelerators can be used for direct electron beam irradiation or to produce X-ray fields *via* the Bremsstrahlung effect, typically involving a tantalum converter.<sup>14</sup>

Both X-ray and gamma rays are photons; however, gamma rays originate from radioactive sources and are emitted during disintegration. Due to their similar nature, the energy deposition patterns (dose profiles) of X-ray and gamma rays are quite comparable, facilitating an easy transition from gamma-ray to X-ray technologies. X-ray may even achieve superior dose uniformity due to specific energy spectrum and easily adjustable radiation field properties.<sup>11</sup> In similarly irradiated materials, e-beams exhibit significantly less penetration compared to photons because their interaction with matter is much stronger. The main difference of the three irradiation technologies is the dose rate.

The role of dose rate in ionizing radiation exposure is complex and multifaceted. In biological systems, the dose rate of ionizing radiation influences a variety of outcomes, from DNA damages and repair mechanisms to cellular responses and whole organism effects.<sup>15</sup> Low-dose-rate (LDR) exposures tend to induce different biological responses compared to high-

<sup>a</sup> Sartorius Stedim FMT S.A.S, Z.I. Les paluds, Avenue de Jouques CS91051, 13781, Aubagne Cedex, France. E-mail: samuel.dorey@sartorius.com

<sup>b</sup> Aix Marseille University, CNRS, ICR, Case 551, 13397 Marseille, France. E-mail: sylvain.marque@univ-amu.fr

<sup>c</sup> Aix Marseille University, Avignon University, CNRS, IRD, IMBE, Marseille, France. E-mail: nathalie.dupuy@amu.fr

<sup>d</sup> Aerial, 250 Rue Laurent Fries, 67400 Illkirch, France

† Electronic supplementary information (ESI) available. See DOI: <https://doi.org/10.1039/d4cp04152f>



dose-rate (HDR) exposures. For instance, LDR radiation can activate adaptive responses that enhance cellular repair mechanisms and reduce mutation rates, while HDR radiation often leads to more immediate and severe damages.<sup>15</sup> Similarly, in polymer systems, the dose rate of ionizing radiation is one of the parameters playing a crucial role in determining the material's properties and performances.<sup>16</sup> Polymers exposed to radiation undergo various chemical and physical changes, such as cross-linking, chain scission, and oxidation. These changes could alter the mechanical, thermal, and chemical properties of the polymer, affecting its suitability for specific applications.

To address these challenges, a multiscale approach is needed, integrating chemical biology, and polymer investigation. This comprehensive strategy will help to bridge the gap between experimental findings on sterilized polymer systems and their applications, providing among others a more accurate understanding of the role of dose rate in ionizing radiation exposure. Recently, the effects of gamma irradiation on the physical/mechanical/chemical properties of a multilayer film composed of EVA/EVOH/EVA were thoroughly studied using various different techniques.<sup>17–27</sup> The impacts of the three irradiation technologies (X-ray, e-beam, and gamma irradiations) have also been investigated by our team.<sup>28,29</sup>

Besides modifications on polymers, other studies highlight that irradiation source and dose rate can influence the formation of transient species and final products.<sup>30</sup> In previous investigation, we showed that transient species generated by gamma rays afford a broad range of molecular species such as carboxylic acids and H<sub>2</sub>O<sub>2</sub>. Combination of these species may highly afford oxidant peracids species spoiling biological solutions. Hence, to model such event, we used the easily and specifically oxidizing methionine proxy.<sup>31</sup>

The oxidation of methionine residues in proteins can have varying effects on protein function. In some cases, it maintains structural integrity and function (cysteine), while in others, it decreases functional activity.<sup>32</sup> Methionine oxidation can alter the structural conformation of proteins, potentially affecting their stability, binding affinity, and overall biological activity. This can compromise the efficacy of therapeutic proteins and antibodies.<sup>33</sup>

In a previous article,<sup>25</sup> it was explained how methionine is oxidized into methionine sulfoxide in gamma irradiated samples and it was shown that if no radical species were detected in the samples, the oxidation was likely due to the presence of hydrogen peroxide, peracids, or *in situ* generated peracids. The effects of X-ray, electron beam, and gamma irradiation on EVA multilayer films at 50 kGy,<sup>28</sup> revealed significant differences in the generation of reactive species among the irradiation technologies. Both gamma and X-ray irradiations produced similar levels of reactive species, while electron beam irradiation resulted in a reduced quantity.

This study aims to compare the effects of three irradiation technologies on polymer modification, providing insights into the attributes of multilayer structures for biopharmaceutical applications and their interactions with biopharmaceutical solutions. Our investigations are focused on how dose rate,

associated with each irradiation technology, on the generation of reactive species such as peroxides and peracids, due to radical post reactivity impact the quality of the materials. It was probed by investigating the nature and amount of generated radical species (electron spin resonance investigation), and by analyzing the oxidation of methionine (high-performance liquid chromatography investigation).

## Materials and methods

### Samples

EVA/EVOH/EVA single-use plastic bags investigated are made from a multilayer film, namely the S71 film, composed of one layer of EVOH sandwiched between two layers of EVA, with a total thickness of approximately 360  $\mu\text{m}$  (Fig. 1). Sample bags are provided by Sartorius Stedim FMT S.A.S, Aubagne, France.

### Packaging

EVA bags were individually wrapped in multilayer packaging (polyethylene/polyamide/polyethylene). Samples were stored in boxes in the dark following irradiation, in an air-conditioned room at  $20 \pm 2$  °C.

### Samples irradiation

**Gamma rays.** EVA/EVOH/EVA bags were irradiated with gamma rays sourced from <sup>60</sup>Co at Ionisos in Dagneux, France, with an average dose rate of 2 kGy h<sup>-1</sup>. There were two irradiation processes: the first spanned over several days, accumulating the dose over multiple runs within the irradiation bunker, while the second was completed in a single run.

EVA bags were also irradiated with gamma rays sourced from <sup>60</sup>Co at Steris in the USA, with an average dose rate of 8 kGy h<sup>-1</sup> (multistep).

### X-ray

EVA/EVOH/EVA bags were irradiated with a 7 MeV Rhodotron at an average dose rate of 80 kGy h<sup>-1</sup> with a maximum power source of 560 kW at Steris, Däniken, Switzerland and also with a 7 MeV Rhodotron, with an average dose rate of 13 kGy h<sup>-1</sup>, at Aerial in Strasbourg, France.

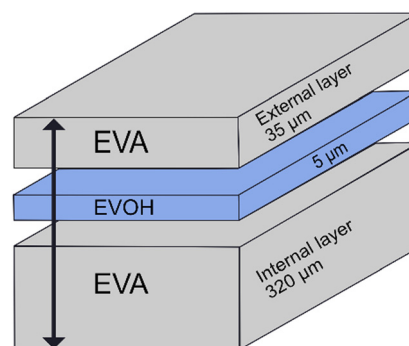


Fig. 1 Representation of EVA/EVOH/EVA multilayer film (S71 film).



**Table 1** Effective doses on samples irradiated by gamma, X-ray, and e-beam for ESR analysis

		Target dose (kGy)	50	100
Received doses (kGy, $\pm 10\%$ )	Gamma	Ionisos, France (1.9 kGy h <sup>-1</sup> )	51	90
	X-ray	Aerial, France (13 kGy h <sup>-1</sup> )	50	99
	e-beam	Aerial, France (18000 kGy h <sup>-1</sup> )	55	109

### e-beam

EVA/EVOH/EVA bags were irradiated with a 10 MeV Rhodotron (Ionisos, Chaumesnil, France) at a dose rate of 18 000 kGy h<sup>-1</sup> with a power source of 28 kW.

EVA/EVOH/EVA bags were also irradiated at Aerial-CRT using the same Feerix<sup>®</sup> facility as the X-ray treatment. A 10 MeV vertical electron beam was utilized, with an average dose rate of 18 MGy h<sup>-1</sup> (5 kGy s<sup>-1</sup>). The irradiation was performed in increments of 50 kGy to prevent critical temperature increases in the samples.

### Dosimetry

The targeted delivered doses were approximately 30, 50, 70 and 100 kGy depending on the irradiation technologies, with a target dose uniformity of  $\pm 10\%$ . There were two phases of irradiation. Table 1 summarizes the dosimetry for the ESR study and Table 2 for the HPLC study. To accurately measure the absorbed dose, alanine pellets combined with ESR spectroscopy (Magnettech MS5000 ESR, Bruker) were used, along with AerEDE<sup>®</sup> dosimetry software (Aerial, France). Dosimetry readings were taken in a manner traceable to an international standard.

### Electron spin resonance (ESR)

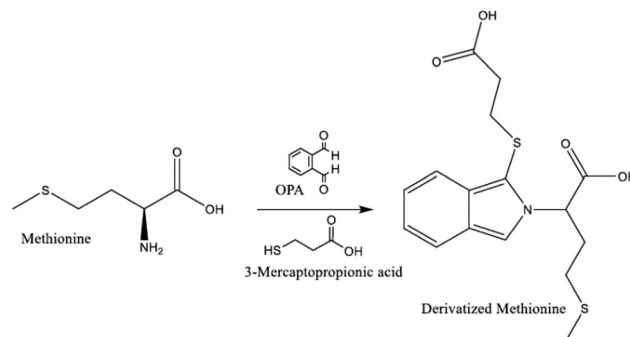
ESR measurements were performed using a Magnettech MS5000X ESR spectrometer, manufactured by Bruker in Switzerland, and operated with ESR studio software for control. More details are given in a previous article.<sup>13</sup>

### High performance liquid chromatography (HPLC)

Three and six months after irradiation, bags were filled with a 50  $\mu$ M solution of methionine in buffer (10 mM NaH<sub>2</sub>PO<sub>4</sub>, 10 mM Na<sub>2</sub>B<sub>4</sub>O<sub>7</sub>·10H<sub>2</sub>O, 5 mM NaN<sub>3</sub>, pH = 8.2). To determine

**Table 2** Effective doses on samples irradiated by gamma, X-ray, and e-beam for HPLC analysis

		Target dose (kGy)	30	50	70	100
d doses (kGy, $\pm 10\%$ )	Gamma	Ionisos, France (1.9 kGy h <sup>-1</sup> )	29	59		
		Ionisos, France (2.4 kGy h <sup>-1</sup> )	32	52		
		Steris, USA (8 kGy h <sup>-1</sup> )	58	54		
	X-ray	Aerial, France (13 kGy h <sup>-1</sup> )	26	51		100
		Steris, Switzerland (80 kGy/h)			68	

**Fig. 2** Automatic derivatization reaction for detecting methionine with a fluorescence detector.

the concentrations of methionine and methionine sulfoxide, an Agilent 1260 HPLC system (Waghaeusel-Wiesental, Germany) equipped with a quaternary pump (G1311C), an autosampler (G1329B), and a fluorescence detector (G1321B) was used. The automated online derivatization (in the autosampler) using an injection program is detailed in Fig. 2. The derivatization reagent used was the *ortho*-phthalaldehyde (OPA).

The gradient program was as follows: 0–13.4 min, 2% phase B; 13.4 min, 57% phase B; 13.5–15.8 min, 100% phase B; 18 min, 2% phase B. Separation was carried out on an Agilent Poroshell HPH-C18 column (4.6 mm  $\times$  100 mm, 2.7  $\mu$ m particles—Waghaeusel-Wiesental, Germany) used with a pre-column,

UHPLC guard Poroshell HPH-C18, 4.6 mm. The column was maintained at 40  $\pm$  0.8  $^{\circ}$ C in a thermostatted column compartment (G1316A) during the analyses. The fluorescence detector was set to an excitation wavelength of 340 nm and an emission wavelength of 450 nm. The total runtime of the method was 20 min. Chromatographic data were acquired and evaluated with the HPLC 1260 OpenLAB software (Waghaeusel-Wiesental, Germany). Internal calibration was done by spiking 20  $\mu$ L of L-Norvaline in each sample and standard.<sup>25</sup>

### Equivalency analysis

Regression models were performed using the Minitab software to assess the effect of doses, the effect of ageing post irradiation, the effect of methionine contact days and the effect of dose rate on the concentration of methionine sulfoxide generated in solution in contact to the multilayer film. This model allows for the evaluation of the significant impact of each independent variable, with confidence interval at 95% ( $\alpha = 0.05$ ).

The Pareto chart shows the absolute values of the standardized effects from the largest to the smallest effect. The chart also plots a reference dotted line indicating if the effects are statistically significant. The reference line for statistical significance depends on the significance level (denoted by  $\alpha$ ), the number of samples, and the degree of freedom.<sup>34</sup>

## Results and discussion

### Electron spin resonance

Fig. 3 displays the ESR detection of radical species in the EVA/EVOH/EVA multilayer film after one and nine days of



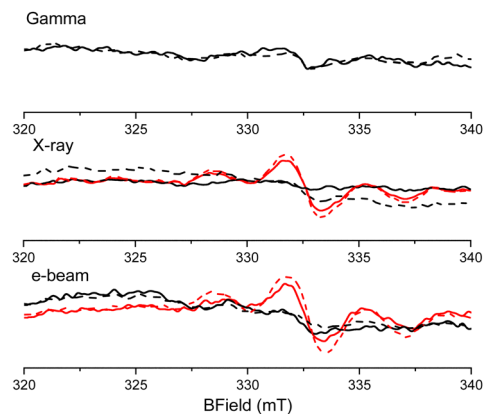


Fig. 3 ESR signal of EVA/EVOH/EVA multilayer film one day (red line) and nine days (black line) after gamma, X-ray and e-beam irradiation at 50 kGy (solid line) and 100 kGy (dashed line).

irradiation. Due to transport time, the sample irradiated by gamma rays cannot be analyzed by ESR one day post-irradiation.

The ESR signals and the monitoring of radical species concentration in the sample post-irradiation reveal that the generated radical species are unstable and can only be quantified one day after irradiation. The amount of radicals observed nine days post-irradiation decreased below the Limit Of Quantification (LOQ) (Fig. S1 in ESI†).

The radical species generated in the EVA/EVOH/EVA multilayer film are identified as hydroxyalkyl radicals in EVOH (Fig. 4), consistent with the literature<sup>28,35</sup> and the different radical pathways are discussed in a previous study.<sup>22</sup>

### Oxidation assay by high performance liquid chromatography

**Comparison of irradiation technology.** In the present study, multilayer films were irradiated at different radiation processing facilities with different dose rates for each irradiation technology, and the quantity of methionine sulfoxide formed was measured three months and six months after irradiation, the methionine sulfoxide concentrations are displayed in Fig. 5.

Regression models were developed to assess whether the dose, ageing post irradiation, methionine contact time and dose rate can have a significant effect on the methionine sulfoxide concentration generated in the multilayer film (Fig. 6).

The results from the regression model, depicted in Fig. 6, indicate that both the contact time with the methionine solution and the dose rate significantly influence methionine oxidation. The equation model is given as (1).

$$\text{Methionine sulfoxide concentration} = 0.676 - 0.00877 \cdot \text{Dose} + 0.0332 \cdot \text{Ageing post irradiation} + 0.1329 \cdot \text{Methionine contact time} - 0.000062 \cdot \text{Dose rate} \quad (1)$$

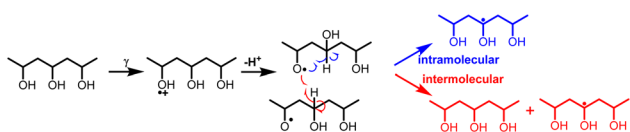


Fig. 4 Different radical pathways to generate hydroxyalkyl radical.<sup>22</sup>

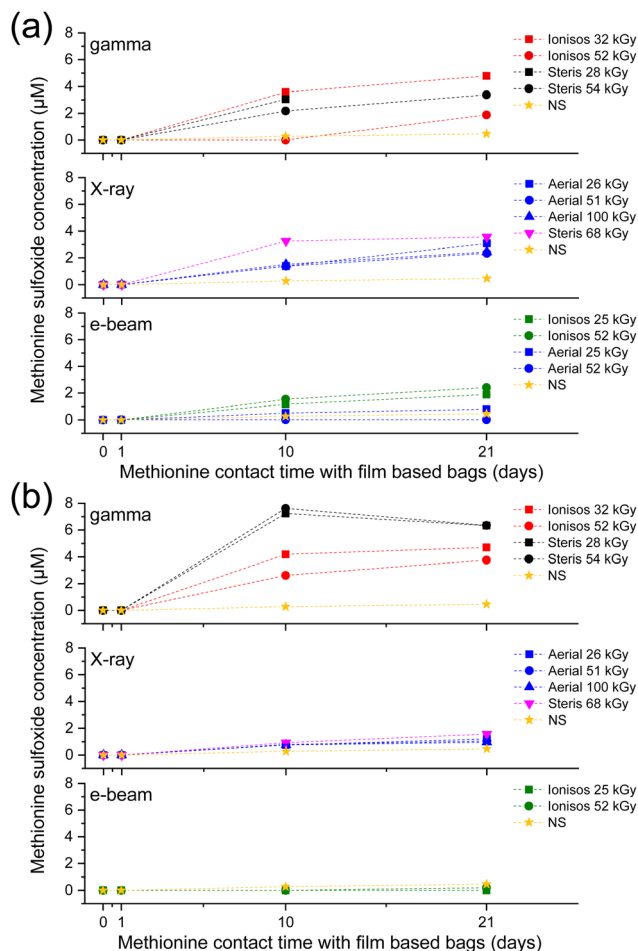


Fig. 5 Bags filled with methionine solution (50  $\mu\text{M}$ ) (a) Three months after irradiation. (b) Six months after irradiation. Methionine sulfoxide concentration in stored solution for 0, 1, 10 and 21 days and analyzed by HPLC. Irradiation doses were 30 kGy (square), 50 kGy (circle), 70 kGy (down triangle) and 100 kGy (up triangle). Non irradiated sample (NS) are in yellow stars. Irradiations at Ionisos, Dagneux, France in red (2  $\text{kGy h}^{-1}$ ), at Steris, USA, in black (8  $\text{kGy h}^{-1}$ ), at Aerial, France in blue (13  $\text{kGy h}^{-1}$  for X-ray and 18 000  $\text{kGy h}^{-1}$  for e-beam), at Steris, Daniken, Switzerland in pink (80  $\text{kGy h}^{-1}$ ) and at Ionisos, Chausmenil, France in green (18 000  $\text{kGy h}^{-1}$ ). Dotted lines have been used for better readability.

The positive coefficient of the contact time indicates that the methionine sulfoxide concentration increased over time when the methionine solution is in contact with the film. This result is in accordance with the Fig. 5.

In this model, the dose rate is influenced by the irradiation technology, as each technology has a specific range of dose rates. Electron beam irradiation uses an accelerator to convert electricity into a radiation beam. The dose rates differ significantly among technologies: gamma rays range from 2 to 8  $\text{kGy h}^{-1}$ , X-rays from 13 to 80  $\text{kGy h}^{-1}$ , and electron beams can reach up to 18 000  $\text{kGy h}^{-1}$ . This higher dose rate of electron beams is directly linked to the irradiation technology, affecting the production of methionine sulfoxide over time when the methionine solution is in contact with the multilayer films. Therefore, the dose rate can be attributed to the irradiation



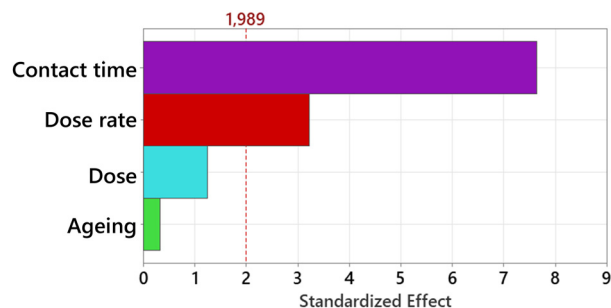


Fig. 6 Pareto analysis of effects on methionine sulfoxide concentration: dose (kGy) (blue), ageing post irradiation (green), methionine contact time (days) (purple) and dose rate (kGy h<sup>-1</sup>) (red). The dotted lines correspond to the significance threshold given by the software MODDE for 95% confidence with  $p$ -value < 0.05.

technology and multilayer films irradiated by gamma radiation generated more methionine sulfoxide.

### Variation of dose rate

A multiparametric regression model was developed for each irradiation technology to assess whether variations in dose rate within the same technology affect the concentration of methionine sulfoxide in methionine solution in contact with the film. For e-beam technology, the dose rate remains similar between the two irradiation sites, thereby preventing any comparison of the dose rate for this technology. The gamma equation model is given as (2) and the X-ray equation model is given as (3).

$$\text{Methionine sulfoxide concentration} = -1.43 - 0.0356 \cdot \text{Dose} + 0.471 \cdot \text{Ageing post irradiation} + 0.2359 \cdot \text{Methionine contact time} + 0.1991 \cdot \text{Dose rate} \quad (2)$$

$$\text{Methionine sulfoxide concentration} = +0.925 - 0.00102 \cdot \text{Dose} - 0.2278 \cdot \text{Ageing post irradiation} + 0.1016 \cdot \text{Methionine contact time} - 0.00652 \cdot \text{Dose rate} \quad (3)$$

In eqn (2) and (3), impact of dose rate is not significant due to very close statistics ( $p$ -value of 0.04 for gamma and  $p$ -value of 0.059 for X-ray) (Fig. 7a and b). Given the limit of 0.05, the results are close for both technologies, and this difference may be attributed to experimental error.

Additionally, the contact time of the methionine solution with the film and the post-irradiation ageing process significantly influence the concentration of methionine sulfoxide due to the oxidant species released by the film for the three irradiation technologies.

### Gamma radiation process

To complete the study, we performed an HPLC investigation to compare two gamma irradiation processes using the same irradiator at Ionisos in France, with a consistent dose rate of 2 kGy h<sup>-1</sup>. The first process involved irradiating the sample in a single run, while the second process accumulated the dose over multiple runs within the irradiation bunker, with unknown rest times between runs.

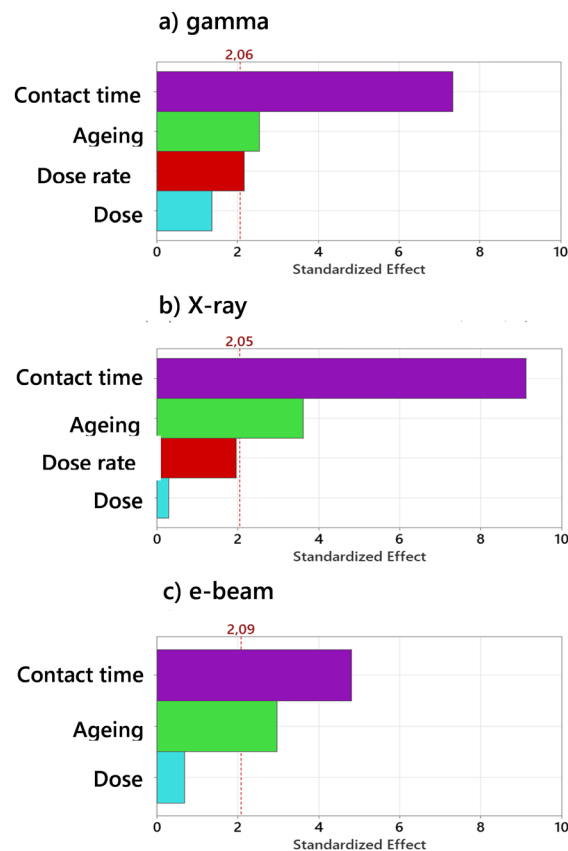


Fig. 7 (a) Multilayer film irradiated by gamma. (b) Multilayer film irradiated by X-ray. (c) Multilayer film irradiated by e-beam. Pareto analysis of effects on methionine sulfoxide concentration: dose (kGy) (blue), ageing post irradiation (green), methionine contact time (days) (purple) and dose rate (kGy h<sup>-1</sup>) (red). The dotted lines correspond to the significance threshold given by the software MODDE for 95% confidence with  $p$ -value < 0.05.

The concentration of methionine sulfoxide formed in the solution in contact with the bag was measured by HPLC in samples after 1, 2, 3, 6, 12, 24, and 36 months irradiation at 30 kGy and 50 kGy (Fig. S2 in ESI†).

A regression model was generated to determine whether the irradiation process, ageing post irradiation, contact time with the solution, and dose had a significant impact on the concentration of methionine sulfoxide formed.

The regression model (Fig. 8) reveals that the contact time with the solution and the multilayer film significantly influence methionine oxidation. Post-irradiation ageing plays a crucial role, indicating that less methionine sulfoxide forms in the solution when the irradiation occurred a long time ago (refer to the coefficient model in the ESI†).

On the other hand, dose and processing have no significant effect on methionine oxidation.

## Conclusion

This study offers insights into the behavior and stability of single-use plastic bags made from EVA/EVOH/EVA multilayer films, extensively used in the biotechnological and pharmaceutical



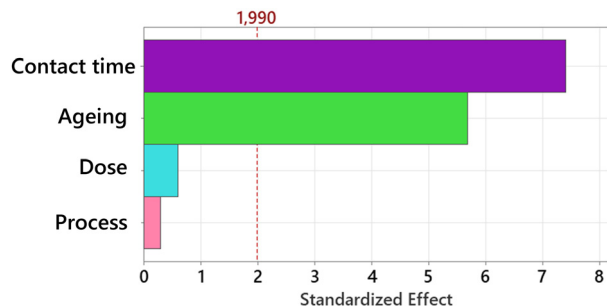


Fig. 8 Pareto analysis of effects on methionine sulfoxide concentration: dose (kGy) (blue), ageing post irradiation (green), methionine contact time (days) (purple) and different process of gamma irradiation (pink). The dotted lines correspond to the significance threshold given by the software MODDE for 95% confidence with  $p$ -value < 0.05.

industries. These materials require sterilization, and the research examined the effects of gamma, X-ray, and electron beam irradiation on these films.

ESR analysis revealed that irradiation generates reactive species such as hydroxyalkyl radicals, which are unstable and can only be quantified one day post-exposure, with concentrations decaying dramatically within nine days. In sharp contrast to the report on PE/EVOH/PE films.<sup>22</sup> The study highlighted that the kinetics and radical species generated are similar for the three irradiation technologies.

The study concludes that the dose rate is one of the parameters which could play a crucial role in the generation of methionine sulfoxide when methionine in solution in contact with the film. This effect is closely related to the irradiation technology used. Notably, the impact of dose rate is not significantly different for X-ray and gamma irradiation. The high dose rate is inherently linked to the e-beam technology.

A regression model examining different gamma irradiation processes reveals that the concentration of oxidized methionine remains statistically equivalent whatever the processes. Post-irradiation ageing significantly affects the results, with materials irradiated 36 months prior exhibiting lower oxidative effects.

These findings highlight the importance of considering dose rate and irradiation technology in optimizing the stability and performance of multilayer films. The research provides valuable insights into the long-term effects of irradiation, guiding future material handling and application strategies.

## Conflicts of interest

There are no conflicts to declare.

## Data availability

The data supporting this article have been included as part of the ESI.†

## Acknowledgements

N. D., F.G. and S. R. A. M. are thankful to Aix-Marseille Université (AMU), Institut de Recherche pour le Développement (IRD) and Centre National pour la Recherche Scientifique (CNRS) for support.

## Notes and references

- J. D. Vogel, The Maturation of Single-Use Applications, *BioProcess Int*, 2012, 10–19.
- E. Mahajan, G. Lye and R. Eibl-Schindler, Bridging polymer Science to Biotechnology Applications: A Single-Use Technology Conference Report, *BioProcess Int*, 2018.
- ISO 11137-1; Sterilization of HealthCare Products-Radiation-Part 1: Requirements for Development, Validation and Routine control of a Sterilization Process for MedicalDevices. ISO: Geneva, Switzerland, 2006.
- Guide to Irradiation and Sterilization Validation of Single-Use Bioprocess Systems, *BioProcess Int*, 2008.
- N. Dupuy, S. R. A. Marque, L. S. Fifield, M. Pharr, D. Staack, S. D. Pillai, L. Nichols, M. K. Murphy and S. Dorey, Supplementing Gamma Sterilization with X-Ray and E-Beam Technologies, *Bioprocess Tech.*, 2022, **20**, 24–28.
- BPAS Technical Guide, X-rays Sterilization of single-Use BioProcess Equipment, Part 1: Industry Need, Requirements & Risk Evaluation, 2021.
- P. M. Armenante and O. Akiti, in *Chemical Engineering in the Pharmaceutical Industry*, ed. D. J. Am Ende and M. T. Am Ende, John Wiley & Sons, Inc., Hoboken, NJ, USA, 2019, pp. 311–379.
- D. Darwis, E. Erizal, B. Abbas, F. Nurlidar and D. P. Putra, Radiation Processing of Polymers for Medical and Pharmaceutical Applications, *Macromol. Symp.*, 2015, **353**, 15–23.
- H. De Brouwer, Comparison of the effects of x-ray and gamma irradiation on engineering thermoplastics, *Radiat. Phys. Chem.*, 2022, **193**, 109999.
- B. Croonenborghs, M. A. Smith and P. Strain, X-ray versus gamma irradiation effects on polymers, *Radiat. Phys. Chem.*, 2007, **76**, 1676–1678.
- T. K. Kroc, Monte Carlo simulations demonstrating physics of equivalency of gamma, electron-beam, and X-ray for radiation sterilization, *Radiat. Phys. Chem.*, 2023, **204**, 110702.
- A. T. Fintzou, A. V. Badeka, M. G. Kontominas and K. A. Riganakos, Changes in physicochemical and mechanical properties of  $\gamma$ -irradiated polypropylene syringes as a function of irradiation dose, *Radiat. Phys. Chem.*, 2006, **75**, 87–97.
- B. Krieguer, S. R. A. Marque, S. Dorey, F. Girard and N. Dupuy, Thermal properties and radical monitoring after gamma, X-ray, and electron beam irradiation in polyamides, *Phys. Chem. Chem. Phys.*, 2024, **26**, 21222–21228.
- G. Sadler, W. Chappas and D. E. Pierce, Evaluation of e-beam,  $\gamma$ - and X-ray treatment on the chemistry and safety of polymers used with pre-packaged irradiated foods: a review, *Food Addit. Contam.*, 2001, **18**, 475–501.
- D. Lowe, L. Roy, M. A. Tabocchini, W. Rühm, R. Wakeford, G. E. Woloschak and D. Laurier, Radiation dose rate effects:



- what is new and what is needed?, *Radiat. Environ. Biophys.*, 2022, **61**, 507–543.
- 16 A. Buttafava, A. Tavares, M. Arimondi, A. Zaopo, S. Nesti, D. Dondi, M. Mariani and A. Faucitano, Dose rate effects on the radiation induced oxidation of polyethylene, *Nucl. Instrum. Methods Phys. Res., Sect. B*, 2007, **265**, 221–226.
  - 17 F. Gaston, N. Dupuy, S. R. A. Marque, M. Barbaroux and S. Dorey, Impact of  $\gamma$ -irradiation, ageing and their interactions on multilayer films followed by AComDim, *Anal. Chim. Acta*, 2017, **981**, 11–23.
  - 18 F. Gaston, N. Dupuy, S. R. A. Marque, D. Gignes and S. Dorey, Monitoring of the discoloration on  $\gamma$ -irradiated PE and EVA films to evaluate antioxidant stability, *J. Appl. Polym. Sci.*, 2018, **135**, 46114.
  - 19 F. Gaston, N. Dupuy, S. R. A. Marque, M. Barbaroux and S. Dorey, FTIR study of ageing of  $\gamma$ -irradiated biopharmaceutical EVA based film, *Polym. Degrad. Stab.*, 2016, **129**, 19–25.
  - 20 S. Dorey, F. Gaston, N. Dupuy, M. Barbaroux and S. R. A. Marque, Reconciliation of pH, conductivity, total organic carbon with carboxylic acids detected by ion chromatography in solution after contact with multilayer films after  $\gamma$ -irradiation, *Eur. J. Pharm. Sci.*, 2018, **117**, 216–226.
  - 21 F. Gaston, N. Dupuy, S. R. A. Marque and S. Dorey, Evaluation of multilayer film stability by Raman spectroscopy after gamma-irradiation sterilization process, *Vib. Spectrosc.*, 2018, **96**, 52–59.
  - 22 G. Audran, S. Dorey, N. Dupuy, F. Gaston and S. R. A. Marque, Degradation of  $\gamma$ -irradiated polyethylene-ethylene vinyl alcohol-polyethylene multilayer films: An ESR study, *Polym. Degrad. Stab.*, 2015, **122**, 169–179.
  - 23 S. Dorey, F. Gaston, S. R. A. Marque, B. Bortolotti and N. Dupuy, XPS analysis of PE and EVA samples irradiated at different  $\gamma$ -doses, *Appl. Surf. Sci.*, 2018, **427**, 966–972.
  - 24 S. Dorey, F. Gaston, N. Girard-Perier, N. Dupuy, S. R. A. Marque and L. Delaunay, Effect of gamma irradiation on the oxygen barrier properties in ethyl-vinyl acetate/ethylene-vinyl alcohol/ethyl-vinyl acetate multilayer film, *J. Appl. Polym. Sci.*, 2020, **137**, 49361.
  - 25 N. Girard-Perier, M. Claeys-Bruno, S. R. A. Marque, N. Dupuy, F. Gaston and S. Dorey, Monitoring of Peroxide in Gamma Irradiated EVA Multilayer Film Using Methionine Probe, *Polymers*, 2020, **12**, 3024.
  - 26 N. Girard-Perier, F. Gaston, N. Dupuy, S. R. A. Marque, L. Delaunay and S. Dorey, Study of the mechanical behavior of gamma-irradiated single-use bag seals, *Food Packag. Shelf Life*, 2020, **26**, 100582.
  - 27 F. Gaston, N. Dupuy, N. Girard-Perier, S. R. A. Marque and S. Dorey, Investigations at the Product, Macromolecular, and Molecular Level of the Physical and Chemical Properties of a  $\gamma$ -Irradiated Multilayer EVA/EVOH/EVA Film: Comprehensive Analysis and Mechanistic Insights, *Polymers*, 2021, **13**, 2671.
  - 28 N. Girard-Perier, S. R. A. Marque, N. Dupuy, M. Claeys-Bruno, F. Gaston, S. Dorey, L. S. Fifield, Y. Ni, D. Li, W. K. Fuchs, M. K. Murphy, S. D. Pillai, M. Pharr and L. Nichols, Effects of X-Rays, Electron Beam, and Gamma Irradiation on Chemical and Physical Properties of EVA Multilayer Films, *Front. Chem.*, 2022, **10**, 888285.
  - 29 B. Krieguer, S. R. A. Marque, S. Dorey, F. Girard, Y. Ni, D. Li, M. K. Murphy, L. S. Fifield and N. Dupuy, Comparison of effects from gamma, e-beam and X-ray radiation on multilayer polymer films used in biopharmaceutical devices by chemometric treatment of spectroscopic data, *Radiat. Phys. Chem.*, 2024, **218**, 111607.
  - 30 T. Pędzinski, K. Grzyb, K. Skotnicki, P. Filipiak, K. Bobrowski, C. Chatgililoglu and B. Marciniak, Radiation- and Photo-Induced Oxidation Pathways of Methionine in Model Peptide Backbone under Anoxic Conditions, *Int. J. Mol. Sci.*, 2021, **22**, 4773.
  - 31 V. Gold, *The IUPAC Compendium of Chemical Terminology: The Gold Book*, International Union of Pure and Applied Chemistry (IUPAC), Research Triangle Park, NC, 4th edn, 2019.
  - 32 M. A. Rosenfeld, L. V. Yurina and A. D. Vasilyeva, Antioxidant role of methionine-containing intra- and extracellular proteins, *Biophys. Rev.*, 2023, **15**, 367–383.
  - 33 D. Tavella, D. R. Ouellette, R. Garofalo, K. Zhu, J. Xu, E. O. Oloo, C. Negron and P. M. Ihnat, A novel method for in silico assessment of Methionine oxidation risk in monoclonal antibodies: Improvement over the 2-shell model, *PLoS One*, 2022, **17**, e0279689.
  - 34 Minitab Statistical software, 2022. Minitab Help. Retrieved from <https://support.minitab.com/en-us/minitab/21/help-and-how-to/>.
  - 35 A. G. Davies, J. A. Howard and M. Lehnig, *Magnetic properties of free radicals- Organic O-, P-, Se-, Si-, Ge-, Sn-, Pb-, As-, Sb-Centered Radicals*, 1979, vol. 9.

